Available online at www.sciencedirect.com

SCIENCE DIRECT®

International Journal of Heat and Mass Transfer 47 (2004) 5201–5210

International Journal of HEAT and MASS TRANSFER

www.elsevier.com/locate/ijhmt

Effects of fuel properties on the combustion behavior of different types of porous beds soaked with combustible liquid

Christopher Y.H. Chao *, J.H. Wang, Wenjun Kong

Department of Mechanical Engineering, The Hong Kong University of Science and Technology,
Clear Water Bay, Kowloon, Hong Kong, China

Received 17 November 2003; received in revised form 2 July 2004

Abstract

Experimental studies were conducted to investigate the behaviors of non-spread diffusion flames of liquid fuel-soaked porous beds. The effects of the properties of the porous bed and the fuel on combustion behaviors, including flame temperature profiles, combustion duration time, fuel consumption and the amount of fuel residue in the porous beds, were studied in the experiments. Additionally, a heat transfer model was used to predict the amount of fuel consumption in the porous beds. Consistency between the predicted and experimental results confirmed that heat conduction is the controlling mechanism in the combustion behavior of liquid fuel-soaked porous beds.

Keywords: Fuel-soaked porous bed; No-spread diffusion flame; Combustion behavior

---

1. Introduction

Knowledge of the combustion behavior of liquid fuel-soaked porous beds is crucial in the application of combustion techniques in soil decontamination and in the prevention of fire in liquid fuel-soaked beds. A number of studies on this subject have been performed [1–13]. In these studies, many efforts focused on the spread of flames over fuel-soaked porous beds [1–9]. Ishida [1,3,8,9] studied the fundamental characteristics of the spread of flames over fuel-soaked glass-bead bed. Experimental results showed that the rate of the flame spread over the ground was considerably slower than that over the surface of a pool of liquid fuel. Takeno and Hirano [2,4] showed that the flame spread over a glass-bead bed is related to the bead diameter and the viscosity of the liquid fuel. Suzuki et al. [5–7] studied the effects of opposed airflows on the flame spread over fuel-soaked sand beds. It was found that a reverse flow helps to stabilize the diffusion flame and assists in the heat transfer from the hot gas to the fuel-soaked beds. Among previous studies on fuel-soaked combustion, only a few studies [10–13] were carried out to understand combustion behaviors, including the burning time, the moving speed of the vapor in the porous bed, and the influence of the depth of the porous bed on diffusion flame characteristics. These aspects are of interest in practical fire prevention because not all of the fuel can be consumed during the combustion process and a significant amount of residue may be left behind in some cases. The residue can trigger another fire if it is not treated properly. Similarly, information about these aspects, particularly fuel consumption rates under different situations, is useful

---

[*] Corresponding author. Tel.: +852 2358 7210; fax: +852 2358 1543.

E-mail address: meyhchao@ust.hk (C.Y.H. Chao).

0017-9310/$ - see front matter © 2004 Elsevier Ltd. All rights reserved.
doi:10.1016/j.ijheatmasstransfer.2004.07.004

Nomenclature

h	depth of the porous bed
L_v	latent heat of evaporation
q	heat flux
t	time
T_a	ambient temperature
T_c	boiling point of liquid fuel
T_{co}	temperature in the liquid–vapor coexisting region
T_l	temperature in the liquid-only region
y_c	interface between the liquid–vapor and the liquid-only regions
y_t	interface between the vapor-only and the liquid–vapor coexisting regions

Greek symbols

α_{co}	thermal diffusivity of the liquid–vapor co-existing region
α_l	thermal diffusivity of the liquid-only region
λ_{co}	thermal conductivity of the liquid–vapor coexisting region
λ_l	thermal conductivity of the liquid-only region
ε	porosity
ρ_l	density of the liquid fuel

in the use of combustion techniques to clean soil. Takeuchi et al. [10] studied the effect of soil properties on the burning characteristics of fuel-soaked porous beds using glass beads saturated with liquid methanol. The consumption rate of methanol and the temperature in the porous bed were measured. Kong et al. [11,12] extended Takeuchi et al.'s study [10] and used sand as the porous bed soaked with liquid methanol to study the combustion behavior in greater detail. Their work showed that the bed depth and sand diameter affect the moving speed of the vapor, the combustion duration time, the fuel consumption and the amount of fuel residue in the fuel-soaked sand bed.

Not much work has been done to understand the influence of fuel properties on combustion behaviors in different types of porous beds. Intuitively, volatility and the boiling point of the liquid fuel should have strong effects on the mass burning rate of the fuel held by the porous media. The purpose of the present study is to investigate in detail the effects of fuel properties on the combustion behavior of liquid fuel-soaked porous beds of different materials that exhibit vast differences in thermal properties and pore characteristics. This study focuses on the non-spread diffusion flame configuration such that some fundamental aspects of combustion behavior can be explored.

2. Experimental

Laboratory-scale experiments were conducted. The schematic view of the experimental set-up is shown in Fig. 1.

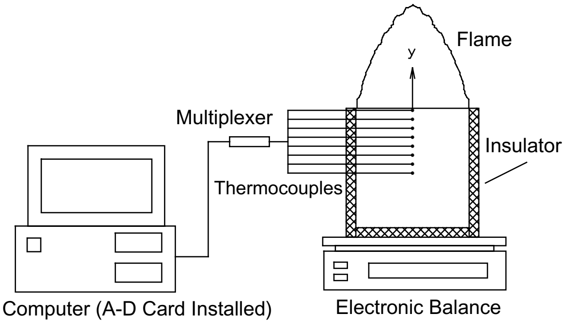

Fig. 1. Schematic diagram of the experimental apparatus.

An insulated stainless-steel cylindrical vessel with an internal diameter of 85 mm, a height of 85 mm and a wall thickness of 1 mm was used to hold the porous material. All the external surfaces of the stainless-steel vessel were enclosed with a 10 mm-thick Kaul wool material to prevent heat loss. In our previous work [11–13], the influences of the diameter of the porous medium and the bed height on the burning characteristics have been discussed. Sands with nine different diameters in the range of 0.12–3.18 mm were used. The results showed that the sand diameter and the height of the porous bed have significant influences on the combustion behaviors. When fuel is accidentally spilled onto the porous ground, it is good to decontaminate the ground by the combustion method if the diameter of the porous medium is fine or if the saturation of the fuel is shallow. The detailed effects of the size of the porous material and the bed depth will not be discussed here again. Only one size with mean diameter of 2.0 mm and one bed depth of 80 mm were used in the present experiments to investigate the effects of fuel properties on the combustion behaviors of different types of porous beds. Here, sand, steel beads and zeolite were used as the porous materials due to their different thermal properties and pore characteristics. The thermophysical properties of the porous materials are listed in Table 1.

Table 1
Properties of liquid fuels and porous beds

Liquid fuels	Chemical formula	Flash point (°C)	Boiling point (°C)	Density (kg/m^3)
(a) Liquid fuels				
Methanol	CH_3OH	11	64.7	791
Ethanol	C_2H_5OH	13	78	789
1-Propanol	C_3H_7OH	15	97	804
2-Butanol	C_4H_9OH	24	99	808
Pentanol	$C_5H_{11}OH$	33	138	800
(b) Porous beds				
Porous beds	Density (kg/m^3)	Specific heat (J/kg K)	Thermal conductivity (W/m K)	Thermal diffusivity (m^2/s)
Sand	2234	710	1.87	1.18×10^{-6}
Steel Bead	7854	434	60.5	1.77×10^{-5}
Zeolite	725	1040	0.2	2.65×10^{-7}

The porous volumes of the sand and steel bead beds are formed mainly by packing the materials in the vessel. However, zeolite exhibits extremely different porous characteristics. Apart from the packed voids, there are quite a lot of inner voids formed while binding the powders of crystalline zeolite into polycrystalline pellets. During the experiments, the porous material was filled into the stainless-steel vessel until the porous bed approached the desired height to guarantee the same container lip height of 5 mm. The container lip affects the flame characteristics in two ways. One is that the flame first heats the lip and the wall transfers the heat by conduction to the porous medium and preheats the vapor. The other is that the container lip leads to quenching of the flame particularly during the extinguishing phase. The same lip height was used to ensure that the effect of the container lip on the combustion behavior was more or less the same in each case.

The combustible liquids used in the experiments were methanol, ethanol, 1-propanol, 2-butanol and pentanol. The properties of these liquids are listed in Table 1. In order to have perfect mixing of the liquid fuel inside the porous beds, the liquid fuel was poured into the porous bed until the liquid was just flush with the bed surface. An electronic balance connected by RS232 to a personal computer recorded the mass of the whole setup automatically and continuously. The temperatures in the porous bed were measured by an array of five K-type thermocouples, all with a sheath diameter of 0.5 mm. In order to obtain the axial temperature profiles during combustion, all the thermocouples were embedded in the vessel with their joint points located at the center axis of the vessel at different locations, $y = -2$, -12, -22, -32, and -52 mm, where y was the distance measured upward from the surface as shown in Fig. 1. In order to minimize the ambient influence on the thermocouple reading, $y = -2$ mm was chosen to measure the temperature of the location nearest the surface, where the thermocouple was embedded just beneath the surface and only a grain size space was chosen for the first spacing. All the combustion experiments were carried out under a quiescent environment with an ambient temperature of about 24 °C and a relative humidity of about 64%. At the beginning of the experiments, ignition was initiated by a pilot flame over the porous bed surface. The experiments were stopped after the flame was extinguished naturally.

3. Results and discussion

3.1. Flame appearances

The ignition processes were not the same for different liquid fuels. Flames spread immediately over the whole bed surface after methanol, ethanol or 1-propanol was ignited. Ignition of 2-butanol was immediate and happened in the position where the pilot flame appeared, and after one second, the flame covered the whole container surface. However, the ignition process of pentanol was slow. The pilot ignition source was used for about 15 s to ignite pentanol, and 30 s later the flame covered the whole container surface. These different ignition processes can be explained by the flash points of the liquid fuels. The flash point is the lowest temperature at which a liquid can form an ignitable mixture in the air near the surface of the liquid. The lower the flash point, the easier it is to ignite the material. Table 1 shows that the flash points of methanol, ethanol and 1-propanol are respectively lower than the ambient temperature. Therefore, sufficient fuel vapor is evaporated from the liquid and the ignition is easy for methanol, ethanol and 1-propanol. The flash point of 2-butanol is the same as the ambient temperature. Once the pilot flame approaches the fuel surface, ignition happens and then the flame immediately heats the nearby fuel to evaporate enough vapor for combustion. The flash point of pentanol is 33 °C, which is higher than the ambient temperature. The pilot flame will first heat the fuel to attain the flash point and then ignite the fuel. The flame continues to heat the nearby fuel to produce enough fuel vapor for the subsequent combustion process. Therefore, the ignition process of pentanol is slower compared to other fuels.

The flames of all the five liquid fuels flickered due to the effect of gravity even in the quiescent environment. The flickering frequencies were about 10 Hz. The flame shapes were almost conical. The flame height for methanol was about 150 mm, and the flame heights for ethanol, 1-propanol, 2-butanol and pentanol were about 200 mm. In each experiment, as combustion proceeded, the flame height increased immediately to its maximum height and then decreased gradually to approach the bed surface and gradually flattened. As time went on, part of the bed surface was not covered with the flame anymore. The extinction first happened at the center of the bed surface. Before extinction, there was only a weak flattened blue flame flickering on the bed surface in a shape of the ring. The appearance of the flame seemed to be very similar among the five liquid fuels. In the experiments, the wall of the vessel could transfer the heat by conduction to the porous bed to preheat the vapor. The external surface of the container was insulated to prevent heat loss and the vapor could thus transfer to the surface near the wall easily to sustain the combustion. This is why the extinction first appeared at the center of the vessel.

It was observed that the flame behavior was slightly different in each porous bed. In the steel bead bed, the combustion process was more vigorous than the processes in the sand and zeolite beds. The flame in the zeolite bed behaved weakly after the ignition. This may be explained by the different thermal diffusivities of the three porous materials, which are listed in Table 1. The thermal diffusivity of the steel bead bed was about 10 times greater than that of the sand bed, which was about five times larger than that of the zeolite bed. Materials with greater thermal diffusivity respond quickly to changes in the thermal environment, while materials with small thermal diffusivity respond more sluggishly. In a liquid fuel-soaked porous bed, after ignition, the liquid fuel is evaporated due to the heat transfer from the flame to the porous bed. The combustion is sustained by the evaporated fuel from the porous bed. Thus quick thermal response of the porous bed can evaporate more fuel to sustain the combustion process.

The liquid fuels exhibited different flame colors during burning. The methanol flame was blue. As burning continued, the blue was mixed with a bit of yellow. The ethanol flame was blue after ignition. After about 3 s, the flame color changed from blue to bright yellow. However, the color at the bottom of the flame near the container lip was still blue. About 3 s after ignition of 1-propanol and 2-butanol flames, the whole flame color changed from blue to bright yellow. The pentanol flame did not cover the whole container surface in the initial phase and the color of the upper portion of the flame was yellow. After the flame developed over the whole porous bed surface, the color became bright yellow. Soot was seen at the flame tips of 2-butanol and pentanol. As the combustion intensity weakened, the flame became blue again in all cases. After the flame was extinguished completely, the porous bed surface was covered with a thin layer of carbon black when 2-butanol and pentanol fuels were used. The color of the flame depends mainly on the chemical and the transport features of the combustion process. The chemical feature is closely related to the oxygen supplements to the fuel. The blue color implies that no soot is emitted from the flame. There are two possibilities for this. Firstly, it is generally agreed that soot is formed in diffusion flames over a limited range of temperature, i.e., $1300\,\mathrm{K} < T < 600\,\mathrm{K}$ [14,15]. Therefore, at the beginning stage of combustion, one possible reason of the appearance of the blue flame is that the flame temperature may not be high enough to trigger the soot formation. The second possibility is that the combustion was completed due to the supply of oxygen. Methanol molecules have one carbon atom. This single carbon is easy to burn completely. Thus, the methanol flame was mainly blue in our experiment. Yellow suggests that soot is formed in the flame. As combustion proceeds, the combustion temperature is high enough to exceed the threshold value of soot formation, which results in the yellow flame. It is difficult to burn 2-butanol and pentanol completely as there are additional carbon atoms in the molecules. Therefore, after the extinction, carbon black was found on the surface of the porous bed when 2-butanol and pentanol fuels were used.

3.2. Temperature distribution in the porous bed

Figs. 2–4 show the temperature profiles in the porous beds soaked with methanol. All the temperatures in the beds first increased rapidly, but the rate of increase slowed down at around the boiling point, and then the temperature increased rapidly again to attain the maximum values. After that, the temperature decreased until spontaneous extinguishment. These temperature characteristics were discussed in our previous papers [11–13]. The temperature retardation occurring at the boiling points of the liquid fuels is at the point of the liquid–vapor coexistence. The abrupt increase of temperature indicates the completion of the liquid fuel evaporation at the location of the thermocouple. This suggests that the region in which the temperature is higher than the boiling point is a vapor region. The point at which there is an abrupt increase of the temperature to the boiling point signifies the lower boundary of the vapor region.

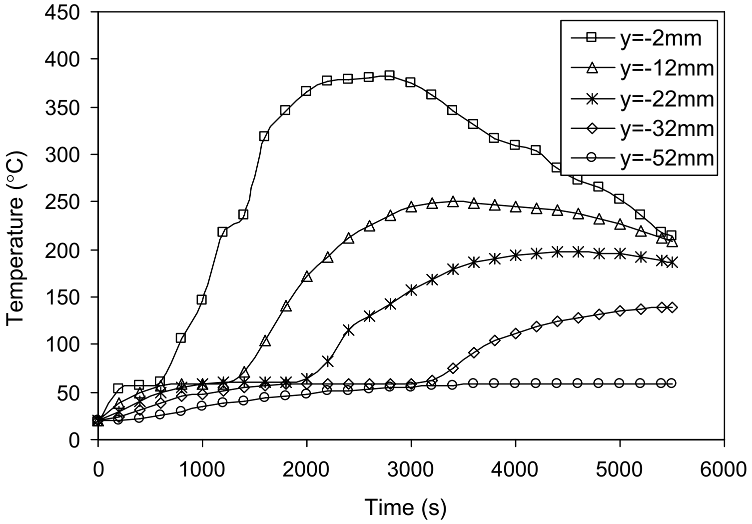

Fig. 2. Temperature profiles in the sand bed soaked with methanol.

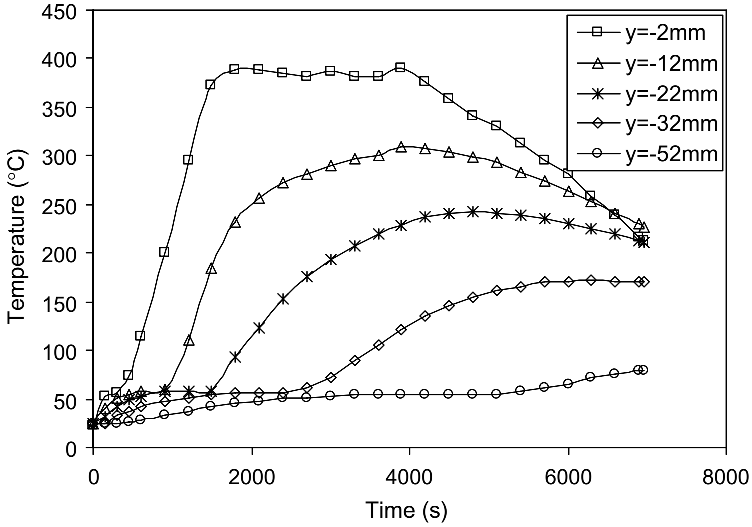

Fig. 3. Temperature profiles in the steel bead bed soaked with methanol.

Fig. 5 shows the temperature–time relationship of methanol in the three porous beds at the location $y = -2$ mm near the surface. The time corresponding to the abrupt increase in temperature to the boiling point was the shortest in the steel bead bed and was the longest in the zeolite bed, i.e., the arrival at the lower boundary of the vapor region in the steel bead bed was the fastest and was the slowest in the zeolite bed. Combustion near the surface of a liquid fuel-soaked porous bed can be influenced by the supply rate of liquid fuel from the porous bed, the heat loss from the bed surface to the environment and the heat transferred to the interior of the porous bed in order to evaporate the liquid fuel. As discussed in our previous papers [11–13], the supply rate of the liquid fuel from the porous bed is by capillary force, which is inversely proportional to the diameter of the porous material. Sand and steel beads have more simple porous structures. However, it should be noted that the zeolite pellets used in the experiments were made by binding crystalline zeolite power into a polycrystalline pellet that contained many subvoids on the magnitude of 100~500 μm inside which there were channels on the nano-scale. Therefore, inside the zeolite bed, besides the pores caused by the packed

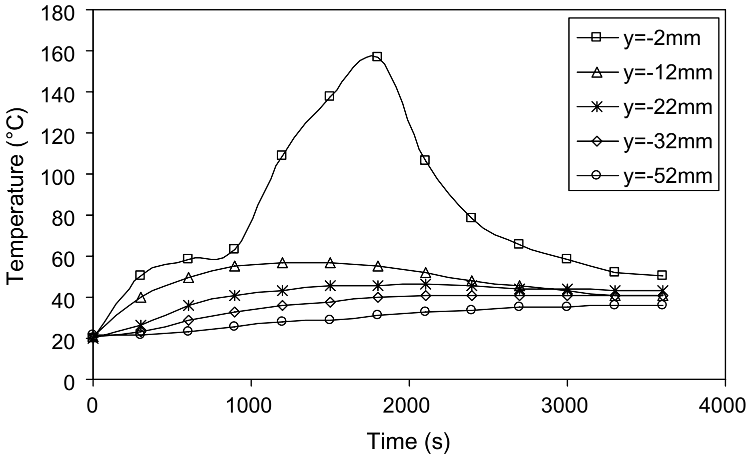

Fig. 4. Temperature profiles in the zeolite bed soaked with methanol.

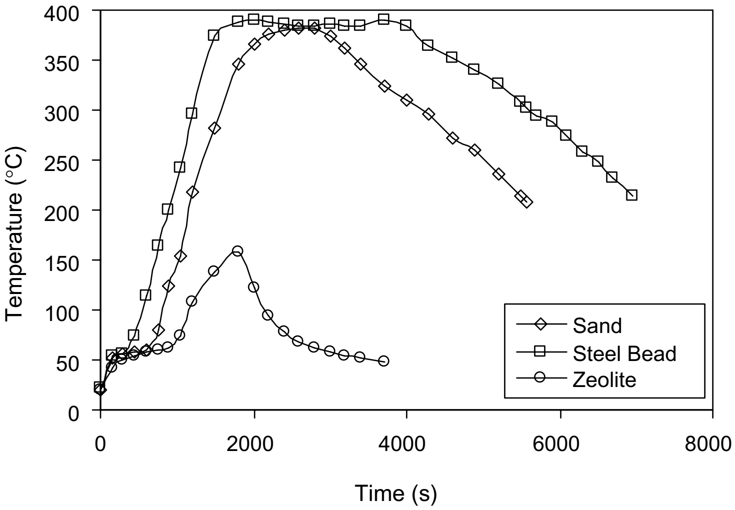

Fig. 5. Temperature vs. time for methanol held by different porous beds at the nearest surface location of $y = -2$ mm.

zeolite pellets, the sub-voids of smaller sizes inside the zeolite pellets could hold more liquid fuel than could the sand and steel bead beds. However, the fuels may not easily leave the zeolite bed as they are held by much stronger adsorption force even though a stronger capillary force should exist for smaller sub-void sizes. The heat transferred from the flame finally evaporates the supplied liquid fuel. A porous material with larger thermal diffusivity can have more heat transferred in a unit time. Thermal diffusivities of the three porous materials are listed in Table 1. During the combustion process, heat loss from the surfaces of the three porous beds to the environment depends on the surface temperature and emissivity. The combustion process is a complicated function of fuel supply from the soaked bed, heat transfer from the flame to the fuel via the porous bed through heat conduction and heat loss to the ambient air. Fig. 5 suggests that the combustion mechanism in the liquid fuel-soaked porous beds could be mainly determined by heat conduction inside the porous bed. Compared to the heat conduction mechanism, heat loss from the bed surface and capillary force by the porous materials seem to play less significant roles.

Similar temperature profiles were found for the other tested liquid fuels in the three kinds of porous beds.

3.3. Propagation speed of the vapor

The temperature profiles at the different locations show that the lower boundary of the vapor region moved downwards in the porous bed as combustion proceeded. The speed of movement of the vapor region inside the porous bed can be calculated from the distance between two consecutive thermocouples and the time interval of the arrival of the lower boundary of the vapor region at the two thermocouple locations. Fig. 6 shows the propagation speed of the vapor region in the sand bed for the different fuels. It is seen that the propagation speed of the vapor inside the sand bed was not constant. The maximum propagation speed for pentanol was in the region from $y = -2$ to -12 mm, while the maximum propagation speeds of the other four fuels occurred in the region from $y = -12$ to -22 mm.

The porous bed material also affects the propagation of the vapor. Fig. 7 shows the arrival of the lower boundary of the vapor region in the three porous beds. At the same location inside the bed, the arrival time in the steel bead bed was the shortest.

As combustion continues, heat from the flame is transferred by conduction to the interior of the porous bed to evaporate the liquid fuel. Thus, Fig. 7 provides further evidence that heat conduction in the porous bed is the dominant factor affecting the combustion behavior of the liquid fuel-soaked porous beds.

3.4. Combustion time

Table 2 summarizes the combustion duration time for different fuels that saturated the three porous beds. The combustion times of 1-propanol and 2-butanol were longer than those of the other fuels. The fuels in the zeolite beds were extinguished more rapidly than those in the sand and steel bead beds. Fig. 4 shows that the liquid fuels at the $y = -12$ mm location could not reach the boiling point in the zeolite bed. Thus, after ignition, the flame reached the maximum temperature and then extinguished rapidly. These experiments seem to suggest that zeolite may be considered as thermal insulation and can be used to extinguish pool fires.

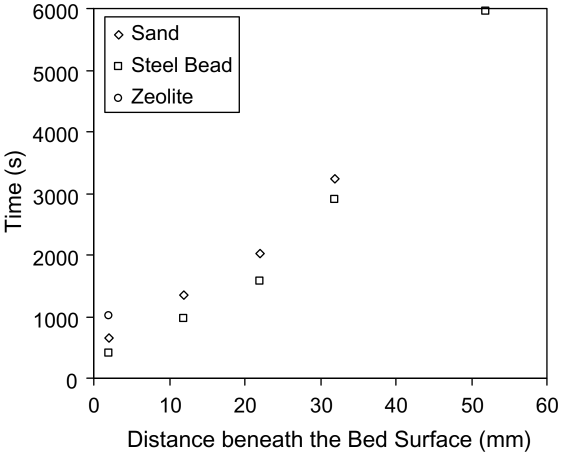

Fig. 7. Arrival time of the lower boundary of the vapor region in the different porous beds.

3.5. Fuel consumption

Before the fuel was ignited, the weights of the liquid fuel and the porous material in each experiment were measured. It was found that the initial weight ratios of

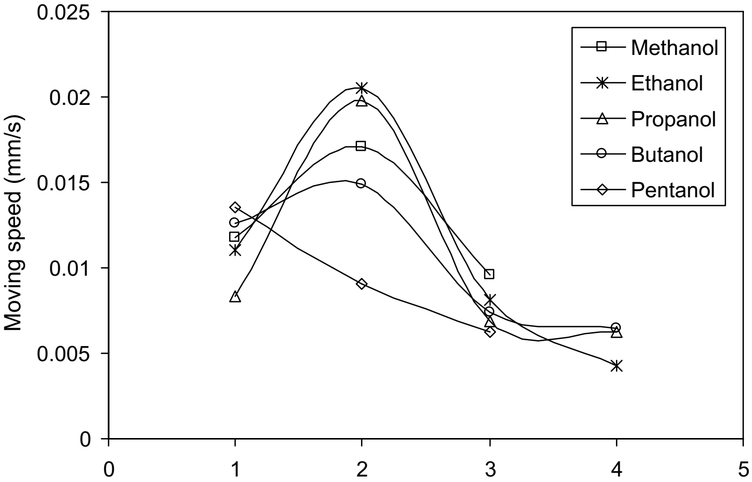

Fig. 6. Propagation speed of the vapor region in the sand bed for different fuels (the value of the horizontal axis denotes the region of two consecutive thermocouples. For example, “1” denoted the region from $y = -2$ to -12 mm, “2” denoted the region from $y = -12$ to -22 mm, etc.).

Table 2
Combustion time and consumption of the liquid fuels held by the porous beds

Porous beds		Methanol	Ethanol	1-Propanol	2-Butanol	Pentanol
Sand	Combustion time (s)	4550	7408	8110	7903	6182
	Original fuel content (g)	175.5	173.6	176.0	193.9	148.5
	Final fuel residue (%)	28.9	10.2	9.38	17.07	19.4
Steel bead	Combustion time (s)	6956	8776	9895	10461	6162
	Original fuel content (g)	163.5	164.3	167.0	168.8	104.3
	Final fuel residue (%)	17.5	4.1	3.1	9	18.7
Zeolite	Combustion time (s)	3770	3900	5100	5089	4800
	Original fuel content (g)	249.6	262.2	284.0	263.0	246.3
	Final fuel residue (%)	73.8	63.5	60.1	63.8	70

the different liquid fuels to the porous material were almost the same for the same kind of porous material. The weight ratios were 0.26, 0.071 and 0.56 for sand, steel beads and zeolite, respectively, regardless of the type of fuel. The fuel consumption (amount of fuel burned) was recorded by an electronic balance connected to a personal computer. Table 2 shows the amount of fuel held by the porous beds prior to ignition and the fuel consumption after combustion. It is seen that the zeolite bed was initially soaked with more fuel than the sand and steel bead beds. Due to the weak combustion behavior in the zeolite bed, after combustion, the ratio of the final fuel residue was far higher than the ratios of the sand and the steel bead beds. About 60∼70% fuel was left un-burned in the zeolite bed.

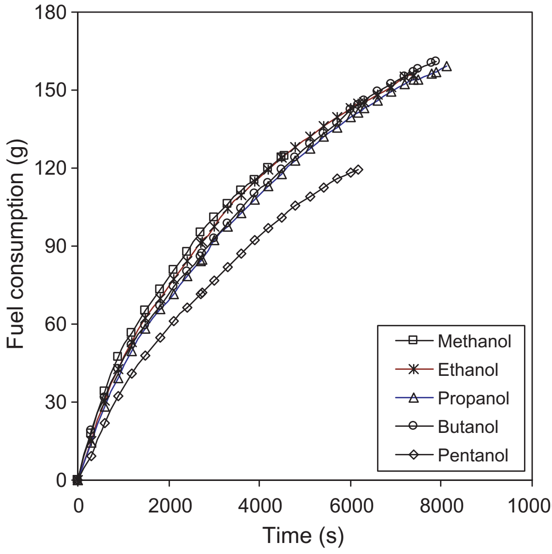

Fig. 8. Fuel consumptions in the sand bed soaked with different combustible liquids.

Fig. 8 shows the fuel consumptions of the different liquid fuels held by the sand bed. It is seen that the fuel consumption gradually decreased with an increase in the flash point of the liquid fuel. The fuel consumption profiles of the other porous beds showed similar patterns.

4. A simple heat transfer model of fuel-soaked combustion

In a liquid fuel-soaked porous bed, the liquid fuel is evaporated due to heat transfer from the flame to the porous bed. The vapor of the liquid fuel diffuses out and reacts with the ambient air, which results in a diffusion flame over the porous bed. In order to account for the aforementioned experimental results, theoretical analysis based on a simple heat transfer model was conducted. The objective of the analysis was to verify that heat conduction is the controlling mechanism of the combustion behavior in the liquid fuel-soaked porous bed. Also, the heat transfer model was adopted to predict the fuel consumption during the combustion process.

Our experimental results suggest that heat conduction is the controlling mechanism of the combustion behavior in a liquid fuel-soaked porous bed. The fuel in the porous bed can be divided into two distinct zones. The upper zone is the liquid–vapor coexisting zone, and the lower region is a liquid zone as shown in Fig. 9. Assuming that heat conduction is the controlling mechanism, the governing equations for the upper region and the lower region are given by

$$\frac{\partial T}{\partial t} = \alpha \frac{\partial^2 T}{\partial y^2}, \quad \text{where } \alpha = \begin{cases} \alpha_{\text{co}}, y_{\text{t}} \leqslant y \leqslant y_{\text{c}} \\ \alpha_{\text{l}}, y_{\text{c}} \leqslant y \leqslant h \end{cases} \tag{1}$$

$$\lambda_l \frac{\partial T_{\text{l}}}{\partial y}\bigg|_{y_{\text{c}}^{+}} - \lambda_{\text{co}} \frac{\partial T_{\text{co}}}{\partial y}\bigg|_{y_{\text{c}}^{-}} = \varepsilon \rho_{\text{l}} L_{\text{v}} \frac{\mathrm{d}y_{\text{c}}}{\mathrm{d}t}, \tag{2}$$

$$T(y_{\text{c}}(t), t) = T_{\text{c}}, \tag{3}$$

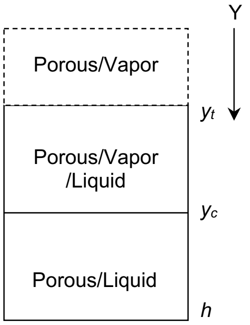

Fig. 9. Schematic diagram of the various zones in fuel soaked combustion.

where y_t is the interface between the vapor region and the liquid–vapor coexisting regions and y_c is the interface between the liquid–vapor and the liquid region.

The boundary condition on the top surface ($y = y_t$) is

$$\lambda_{co}\frac{\partial T_{co}}{\partial y}\bigg|_{y=y_t} = -q, \tag{4}$$

where q is the ignition energy at the beginning of combustion and the heat flux feedback to the surface as the combustion proceeds; it is a variable parameter changing with time. In this paper, we follow [16] and take q to be constant for simplicity.

The boundary condition at the bottom of the porous bed ($y = h$) is

$$\frac{\partial T_l}{\partial y}\bigg|_{y=h} = 0. \tag{5}$$

The initial conditions are:

$$T(y, 0) = T_a, \tag{6}$$

$$y_c(0) = y_t(0) = 0. \tag{7}$$

By using the heat-balance integral method [17], Eqs. (1)–(3) can be simplified to a pair of ordinary differential equations (ODEs). In this approach, the quadratic temperature profiles satisfying the boundary conditions in each zone are assumed.

In the upper zone, i.e., the liquid–vapor coexisting region, the temperature profile is assumed to be:

$$T = T_s - \frac{q}{\lambda_{co}}(y - y_t) + \frac{q - q^*}{2\lambda_{co}(y_c - y_t)}(y - y_t)^2, \tag{8}$$

where T_s is the temperature at the surface $y = y_t$ and q^* is the heat flux just above $y = y_c$.

In the lower zone, i.e., the liquid zone, the temperature distribution is assumed to be:

$$T = T_c - 2(T_c - T_a)\frac{y - y_c}{D} + (T_c - T_a)\left(\frac{y - y_c}{D}\right)^2, \tag{9}$$

where D is the thermal penetration depth defined by the condition that at $y = y_c + D$, $T = T_a$ and $\partial T/\partial y = 0$.

Basing on the assumed temperature profiles, the final equations of the ODEs are presented as:

$$\varepsilon\rho_l L_v \frac{dy_c}{dt} = q^* - 2\lambda_l \frac{T_c - T_a}{D} \tag{10}$$

$$\frac{1}{3}\frac{dD}{dt} + \frac{dy_c}{dt} = \frac{2\alpha_l}{D}. \tag{11}$$

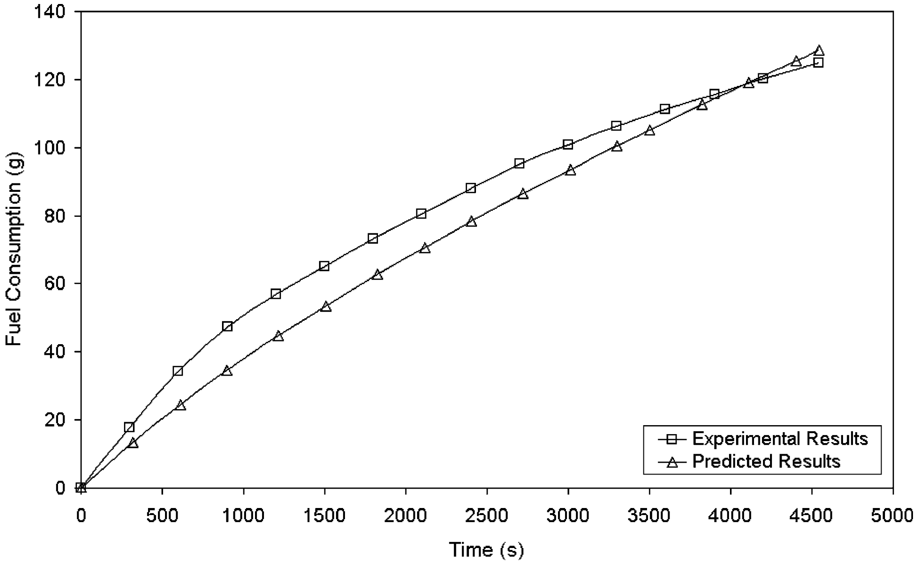

Fig. 10. Comparison of the predicted consumption of methanol in the sand beds with the experimental results.

By solving the ODEs, the fuel consumption in the porous beds can be calculated. It is seen that the predicted fuel consumption is quantitatively consistent with the experimental results. The fuel consumption of methanol in the sand bed is presented in Fig. 10. The used parameter values for methanol are $\lambda_l = 0.195\,\mathrm{W/m\,K}$, $T_c = 337.5\,\mathrm{K}$, $T_a = 298\,\mathrm{K}$, $L_v = 1.099\,\mathrm{MJ/kg}$, $\alpha_l = \alpha_{co} = 1.04 \times 10^{-7}\,\mathrm{m^2/s}$, and $q = 35\,\mathrm{kW/m^2}$ [16]. The porosity of the sand bed is $\varepsilon = 0.46$ [6]. The consistency between the calculated and experimental results shows that heat conduction is the controlling mechanism of the combustion behavior in a liquid fuel-soaked porous bed and the above heat transfer model can be used to predict the amount of fuel consumption in the porous bed.

5. Conclusions

This study described the combustion behaviors of various types of porous beds soaked with different liquid fuels. From the experimental results, it is seen that the combustion processes follow similar patterns. After ignition, flames spread immediately over the whole bed surface, the flame height gradually reached to its maximum value, and then the flame extinguished itself. For the different porous beds, the combustion time, temperature profiles and fuel residue in the beds were dissimilar. Although the original amount of liquid fuels soaked in the zeolite beds was more than that in other beds (the sand and steel bead beds), the combustion time was shorter than the fuels burned in other beds due to its low thermal diffusivity and perhaps also due to the adsorption force holding the fuels in the sub-voids that do not exist in sand and steel beads. Zeolite seems to be a good thermal insulator and can be used as an extinguishing agent to quench liquid pool fires. The experimental results also show that for the liquid fuels soaked in porous beds of high thermal diffusivity, it is preferable to use combustion to decontaminate the beds. According to the theoretical analysis of the combustion behavior in the fuel-soaked porous beds based on a simplified heat transfer model, the presented heat transfer model can be used to predict the amount of fuel consumption in the porous beds. The good consistency between the predicted results and the experimental results showed that heat conduction is the dominant mechanism controlling combustion in the fuel-soaked porous beds.

Acknowledgment

This research was funded by the Hong Kong Research Grant Council under Grant No. HKUST6040/99E.

References

[1] H. Ishida, Flame spread over fuel-soaked ground, Fire Saf. J. 10 (1986) 163–171.

[2] K. Takeno, T. Hirano, Flame spread over porous solids soaked with a combustible liquid, in: Proceedings of the 21st Symposium (International) on Combustion, 1986, pp. 75–81.

[3] H. Ishida, Flame spread over ground soaked with highly volatile liquid fuel, Fire Saf. J. 13 (1988) 115–123.

[4] K. Takeno, T. Hirano, Behavior of combustible liquid soaked in porous beds during flame spread, in: Proceedings of the 22nd Symposium (International) on Combustion, 1988, pp. 1223–1230.

[5] T. Suzuki, M. Kawamata, T. Hirano, Flame spread over fuel soaked sand in an opposed air stream, in: Fire Safety Science – Proceedings of the Second International Symposium, Hemisphere Pub. Corp., New York, 1989, pp. 199–208.

[6] T. Suzuki, M. Kawamata, K. Matsumoto, T. Hirano, Behavior of the reverse flow in front of the leading flame edge spread over fuel-soaked sand in an air stream, in: Fire Safety Science – Proceedings of the Third International Symposium, Elsevier Applied Science, New York, 1991, pp. 227–236.

[7] T. Suzuki, M. Kawamata, K. Matsumoto, T. Hirano, Aerodynamic and thermal structures of the leading flame edge spreading over fuel soaked sand in an opposed air stream, in: ASME/JSME Thermal Engineering Proceedings, ASME, vol. 5, 1991, pp. 341–346.

[8] H. Ishida, Initiation of fire growth on fuel-soaked ground, Fire Saf. J. 18 (1992) 213–230.

[9] H. Ishida, K. Sato, K. Hokari, T. Hara, Flame spread over fuel-spilled and/or snow-asphalt road, J. Fire Sci. 14 (1996) 50–66.

[10] T. Takeuchi, T. Tsuruda, S. Ishizuka, T. Hirano, Burning characteristics of a combustible liquid soaked in porous beds, in: Fire Safety Science – Proceedings of the Third International Symposium, Elsevier Applied Science, New York, 1991, pp. 405–414.

[11] W.J. Kong, C.Y.H. Chao, J.H. Wang, Behavior of non-spread diffusion flames of combustible liquid soaked in porous beds, in: Proceedings of the 29th Symposium (International) on Combustion vol. 29, 2002, pp. 251–257.

[12] W.J. Kong, C.Y.H. Chao, J.H. Wang, Burning characteristics of non-spread diffusion flames of liquid fuel soaked in porous beds, J. Fire Sci. 20 (2002) 203–225.

[13] J.H. Wang, C.Y.H. Chao, Combustion behavior of liquid fuel soaked in porous beds, in: The Third Asia-Pacific Conference on Combustion, Seoul, Korea, 2001, pp. 150–153.

[14] J. Bowen, Dynamics of Exothermicity, Gordon and Breach Publishers, 1996, pp.151–184.

[15] S.D. Watt, J.E.J. Staggs, A.C. McIntosh, J. Brindley, A theoretical explanation of the influence of char formation on the ignition of polymers, Fire Saf. J. 36 (2001) 421–436.

[16] S.R. Turns, An Introduction to Combustion, Concepts and Applications, McGraw-Hill, 2002, pp. 343–346.

[17] T.R. Goodman, The heat-balance integral and its applications to problems involving a change of phase, J. Heat Trans., ASME 80 (1958) 335–342.